

Poly(THF-co-cyano ethylene oxide): Cyano Ethylene Oxide (CEO) Copolymerization with THF Leading to Multifunctional and Water-Soluble PolyTHF Polyelectrolytes

Eva-Maria Christ,^{†,‡} Jana Herzberger,^{†,‡} Mirko Montigny,[§] Wolfgang Tremel,[§] and Holger Frey^{*,†}

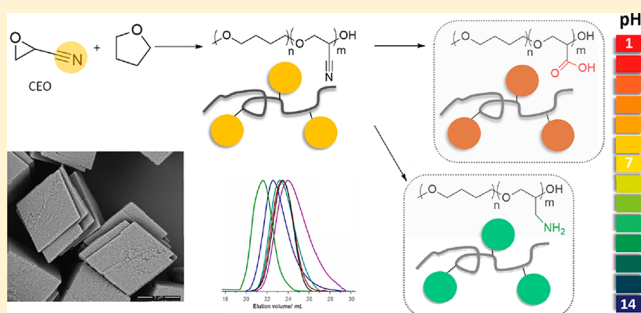
[†]Institute of Organic Chemistry, Johannes Gutenberg-University Mainz, Duesbergweg 10-14, D-55128 Mainz, Germany

[‡]Graduate School Materials Science in Mainz (MAINZ), Staudingerweg 9, D-55128 Mainz, Germany

[§]Institute of Inorganic Chemistry and Analytic Chemistry, Johannes Gutenberg-University, Duesbergweg 10-14, 55128 Mainz, Germany

Supporting Information

ABSTRACT: Cyano-functional polyether copolymers based on THF were prepared via cationic ring-opening copolymerization of THF with cyano ethylene oxide (CEO). The CEO content of poly(tetrahydrofuran) (polyTHF) based copolymers varied from 3.3 to 29.3%, and molecular weights ranged from 5100 to 31900 g·mol⁻¹ with M_w/M_n in the range of 1.31 to 1.74 (SEC in THF, PS standards). The polymerization was conducted with methyl trifluoromethanesulfonate (MeOTf) as an initiator. Kinetic studies concerning incorporation of both monomers were performed via NMR spectroscopy. The cyano groups at the poly(THF-co-CEO) copolymers enable direct access to amino (polyTHF-NH₂) and carboxyl groups (polyTHF-COOH) in facile one-step procedures, respectively. The modified copolymers were characterized via NMR, MALDI-ToF mass, and FT-IR spectroscopy. Thermal properties of the materials were studied via differential scanning calorimetry (DSC), demonstrating a gradual decrease of the melting points with increasing amount of CEO in the copolymers (from 30 °C for 3.3% CEO to 21 °C for 8.4% CEO). After postmodification to carboxylic acid groups the melting points decrease from 26 to 18 °C in the series of copolymers. Contact angles of water on thin films of the polymers can be tuned in a wide range from 72.7° to 17.8° by varying the CEO fraction as well as by postmodification. Crystallization studies of CaCO₃ with water-soluble polyTHF-COOH revealed the composition-dependent inhibition of calcite growth, with crystallite size in the mineralization process being controlled by the amount of carboxylic acid groups at the poly(THF) copolymers.



INTRODUCTION

Poly(tetrahydrofuran) (polyTHF) is an extremely versatile material that is characterized by its remarkably high chain flexibility and its apolar nature.¹ PolyTHF possesses a low melting point (28 °C), which contributes to its easy handling, besides excellent solubility in a wide range of rather hydrophobic solvents like chloroform or THF. This renders the material interesting for manifold applications, e.g., as soft component in the polyurethane production^{2,3} (e.g., for Spandex), for the synthesis of fibers, adhesives, and sealants, and for coatings in the textile industry. Characteristic properties like the high hydrolytic stability in contrast to other polyester polyols, a high moisture vapor transmission, and high abrasion resistance as well as microbial resistance play a key role for these purposes. Furthermore, the resulting materials possess good visible light transparency.^{4,5} Besides its applications in a wide industrial field, polyTHF is also favorable for manifold biomedical applications, such as a key component in contact lenses, due to its low solubility in water and its good biocompatibility.⁴ Last but not least, polyTHF represents a

straightforward “end-of-life polymer”, since it can easily be degraded to THF in a facile and inexpensive way.^{6,7}

The properties of polyTHF can be systematically expanded and manipulated by modification of the end-groups. Rowan et al. reported the synthesis of nucleobase-terminated polyTHF, which self-assembled to materials with film and fiber-forming capability.⁸ By diversifying the initiator of the polymerization, the starting group of polyTHF can be varied as well^{9,10} to create telechelic and heterobifunctional polyTHF.¹¹ The introduction of functional groups, such as alkyl, -OH, -NH₂, -COOH, and -COOR, is an attractive objective, because these moieties can be used to tune the hydrophilic/hydrophobic character, permeability, and mechanical properties, as demonstrated recently for polycarbonates.¹² Also for related hydrophilic polyethers, multifunctionality is generally an important target, as demonstrated in numerous publications in

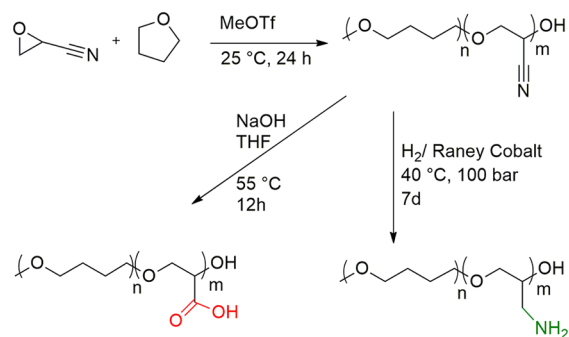
Received: January 16, 2016

Revised: April 21, 2016

recent years.^{13–19} Amine-functional polyTHFs were presented in two works; however, the amino groups were positioned only as end-groups as well.^{20,21} As a further end-group functionalized material, the group of Teixidor provided reversible, redox-active polyTHF by combining polyTHF with metallacarboranes.²² The direct copolymerization of THF with ethylene oxide has been studied, e.g., by Bednarek and Kubisa²³ and later by Höcker et al.,²⁴ and was found to proceed in a random manner. The cationic copolymerization of THF with functional cyclic monomers has been presented in a few intriguing works. In this area, the group of Zhu reported the copolymerization of THF with glycidol to create branched copolymers with numerous hydroxyl groups²⁵ and the group of Pomposo et al. combined THF with glycidyl phenyl and glycidyl propargyl ether,²⁶ based on previous work of Du Prez and co-workers.²⁷ THF was also copolymerized with epichlorohydrin or bis(chloromethyl)-oxetane to create high-energy binders after postmodification, resulting in materials with high nitrogen content.^{28,29}

In the current work we have studied the cationic random (co)polymerization of THF with the novel functional monomer cyano ethylene oxide (CEO) (Scheme 1).

Scheme 1. Copolymerization of CEO and THF, as Well as Post-Modification Reactions, Leading to PolyTHF Copolymers with Carboxylic Acid and Amine Moieties



We demonstrate that the combination of these two monomers results in linear multifunctional polyTHF copolymers with a large number of functional cyano groups (from 3.3 to 29.3%, analyzed via NMR). Comprehensive characterization of all copolymers via MALDI–ToF mass spectrometry, NMR spectroscopy, size exclusion chromatography (SEC), FT-IR spectroscopy, and differential scanning calorimetry (DSC) has been carried out. We also demonstrate that the cyano groups can be postmodified to primary amine groups and carboxylic acid groups, resulting in water-soluble polyTHF at elevated pH. This material has been explored for the mineralization of calcium carbonate, as will be discussed in the final part of this work.

EXPERIMENTAL SECTION

Materials. All reagents were purchased from Acros Organics or Sigma-Aldrich and were used as received, unless otherwise stated. Anhydrous DMSO and *o*-dichlorobenzene were stored over molecular sieves prior to use. Column chromatography was performed on silica gel (particle size 63–200 μm , Merck, Darmstadt, Germany). Deuterated DMSO- d_6 , pyridine- d_5 , MeOD- d_3 , CDCl₃, and HFIP- d_2 were purchased from Deutero GmbH. Tetrahydrofuran (THF) was purified by standard methods and was distilled over sodium in the presence of benzophenone. Dialysis membrane tubings were purchased from Sigma-Aldrich or Orange Scientific, respectively. For dialysis in chloroform, a membrane of regenerated cellulose

(benzoylated) was used. For dialysis in protic solvents, regular regenerated cellulose membranes were applied.

Instrumentation. ¹H NMR (300 and 400 MHz) and ¹³C NMR spectra (75 and 100.6 MHz) were recorded on Bruker AC300, Bruker AC400, Avance III HD 300 (300 MHz, 5 mm BBFO-head with *z*-gradient and ATM, B-ACS 60 sample changer) spectrometers with Open-Access-Automation, Avance II 400 (400 MHz, 5 mm BBFO-head with *z*-gradient and ATM, SampleXpress 60 sample changer) with Open-Access-Automation or Avance III HD 400 (400 MHz, 5 mm BBFO-SmartProbe with *z*-gradient and ATM, SampleXpress 60 sample changer), respectively, and are referenced internally to residual proton signals of the deuterated solvents. ¹H NMR experiments for kinetic studies were acquired with a 5 mm BBFO *z*-gradient probe on the 500 MHz Bruker AVANCE III system. For the respective ¹H NMR spectra, 64 transients were used with a 10.6 μs long 90° pulse and 10000 Hz spectral width together with a recycling delay of 10 s. For the ¹³C NMR kinetic measurements, 32 scans were used with a relaxation delay of 30 s (90° pulse, 13.2 μs , spectra width 30000 Hz). The temperature was kept at 298.3 K and calibrated with a standard ¹H methanol NMR sample using the topspin 3.2 software (Bruker). Control of the temperature was realized with a VTU (variable temperature unit) and an accuracy of $\pm 0.1\text{K}$.

For size exclusion chromatography (SEC) measurements in THF a PU 1580 pump, an auto sampler AS1555, a UV-detector UV 1575 (detection at 254 nm) and a RI-detector RI 1530 from JASCO were used. Columns (MZ-Gel SDplus 10² Å and MZ-Gel SDplus 10⁶ Å) were obtained from MZ-Analysentechnik. Calibration was carried out with polystyrene (PS) standards purchased from Polymer Standard Services (PSS). MALDI–ToF MS measurements were performed on a Shimadzu Axima CFR MALDI-TOF mass spectrometer using dithranol (1,8,9-trihydroxyanthracene) or CHCA (α -Cyano-4-hydroxycinnamic acid) as a matrix. The samples were prepared from pyridine and ionized by adding lithium chloride or potassium trifluoroacetate.

DSC measurements were carried out on a PerkinElmer DSC 8500 in the temperature range of –80 to 50 °C, using heating rates of 10 K min^{–1} under nitrogen. Contact angle measurements were performed on a Dataphysics Contact Angle System OCA using water as an interface agent. SEM images were taken with a FEI Nova NanoSEM at acceleration voltage of 5 kV and a vC detector or a FEI Phenom SEM at 3 kV acceleration voltage, respectively.

TEM images were recorded using a FEI Technai T12 equipped with a 4K CCD camera and a LaB₆ cathode working on 120 kV acceleration voltage. Samples for TEM were prepared by dropcasting 20 μL of the sample dilution from crystallization beakers onto a carbon coated copper grid (Plano GmbH, Wetzlar, Germany).

Raman-spectroscopy measurements for phase identification were carried out using a confocal HR800 μ -Raman by Horiba Scientific. Raman stimulation was managed by exciting with $\lambda = 633,318\text{ nm}$ He/Ne laser without using any filters. To get best signal-to-noise possible a pinhole with a 400 nm diameter has been used. The signal was collected with a CCD detector with a 1024 \times 256 pixels open electrode chip.

Synthetic Procedures. *Synthesis of Cyano Ethylene Oxide (CEO).* CEO was synthesized as described in the literature.³⁰ Briefly, in the course of 3 h at 0 °C, 100 mL of sodium hypochlorite (13% active chlorine) was added with a dropping funnel to cold acrylonitrile (100 mL, 1.53 mol). The mixture was stirred vigorously with a mechanical stirrer at 0 °C for additional 21 h, leading to a yield of 39.5% (Lit.: 34.5%).³⁰ Subsequently, residual acrylonitrile was recovered by distillation, and the product was purified by distillation *in vacuo* (60 °C, 10^{–2} mbar). ¹H NMR (300 MHz, CDCl₃): δ (ppm) = 2.95–3.25(m, 2H, –CH₂–), 3.4–3.54 (m, 1H, –CH). ¹H and ¹³C NMR spectra of CEO are shown in the Supporting Information, Figure S1. To avoid degradation to 3-cyanopropanal, the labile monomer CEO was stored under argon at –18 °C.

Representative Procedure for the Synthesis of Poly(THF-co-CEO) Copolymers. CEO (0.1 g, 1.45 mmol, 69.02 g mol^{–1}) and THF (1.05 g, 14.5 mmol, 72.06 g mol^{–1}) were mixed in a glass tube under argon atmosphere at room temperature. Methyl trifluoromethanesulfonate

Table 1. Characterization Data for the Series of Poly(THF-*co*-CEO) Copolymers Prepared

composition ^a	[CEO]/%	CEO fraction ^a /%	M_n^a /g mol ⁻¹	M_n^b /g mol ⁻¹	M_w/M_n^b
PTHF ₅₈₆	0	0	42200	73000	1.83
P(THF _{146.2} - <i>co</i> -CEO ₅)	5	3.3	10900	18800	1.59
P(THF ₂₈₉ - <i>co</i> -CEO ₁₄)	5	4.6	21800	31900	1.42
P(THF _{174.8} - <i>co</i> -CEO _{11.7})	6	6.3	13400	9800	1.31
P(THF _{118.2} - <i>co</i> -CEO _{8.8})	7	6.9	9100	9700	1.34
P(THF _{120.4} - <i>co</i> -CEO _{11.1})	9	8.4	9400	8600	1.49
P(THF ₅₃ - <i>co</i> -CEO ₂₃)	25	29.3	5300	5100	1.74

^aObtained from ¹H NMR spectra. ^bDetermined by SEC measurements (THF, PS standards, RI signal).

carefully on both sides with saturated CaCO₃ dilution and Millipore-water to ensure resolving ammonium carbonate crystals without inducing the resolving–recrystallization mechanism and to remove excessive unbound polymer followed by drying under airflow.

RESULTS AND DISCUSSION

A. Monomer Synthesis and Copolymerization of CEO with THF. Monomer Synthesis. Cyano ethylene oxide (CEO) can be synthesized in a one step-procedure, following a modified literature protocol.³⁰ Dropping sodium hypochlorite to acrylonitrile affords the desired product. The excess of acrylonitrile can be retrieved by distillation. In this way, the moderate to low yield of the product CEO (39.5%) can be enhanced by utilizing repetitive procedures. To avoid possible degradation of the monomer CEO to 3-cyano propanal, it was stored under argon at −18 °C. To date, CEO has not been employed successfully as a monomer for polymerizations to the best of our knowledge. First attempts to polymerize CEO were described by Wei and Butler in the 1970s, however no polymer could be obtained.³⁶

Copolymerization of THF and CEO. The copolymerization of THF and CEO was carried out with methyl trifluoromethanesulfonate (MeOTf) as an initiator, following recently reported results regarding cationic ROP of THF with MeOTf as an initiator.³⁷ We chose this initiator because of the high reactivity of MeOTf for the initiation of the “living” THF polymerization in a fast and quantitative way.³⁷ The polymerization mechanism of THF with this initiator is known to follow the so-called “active chain end” (ACE) mechanism (Scheme 2) regarding the polymerization of CEO, in accordance to literature describing the polymerization of THF.³⁸ The commonly very powerful methylating agent MeOTf³⁹ methylates the ring system either of THF or CEO to enable the following nucleophilic attack of the oxygen atom at another cyclic monomer. This step can be repeated either with CEO or THF monomers, leading to linear chains. The (co)polymerization can be terminated either with a base, e.g., pyridine or with a protic compound, e.g., methanol or water. Although the homopolymerization of THF is known to follow the ACE mechanism, this is not necessarily the case for the copolymerization of THF with other cyclic monomers.

As stated for the recently published copolymerization of THF and glycidyl phenyl ether with B(C₆F₅)₃ as a catalyst, the (co)polymerization can be controlled by synthesis conditions, such as reaction time, catalyst concentration, and monomer concentration.⁴⁰ However, a high THF content appears to be necessary to avoid cyclic products.⁴⁰ Furthermore, for the (co)polymerization of THF with other cyclic monomers as, e.g., ethylene oxide or the bisglycidyl ether of bisphenol A it appears to depend on reaction conditions, whether the ACE mechanism or the “Active Monomer” (AM) mechanism

occurs,⁴¹ however this was observed only for other catalysts and not for MeOTf.^{23,24,42–44} Finally, the polymerization of ethylene oxide is known to follow the AM mechanism with Broensted acids as a catalyst, in contrast to the polymerization of THF.²⁹ On the basis of this knowledge, we expected to observe coexistence of both mechanisms in the copolymerization of THF with CEO.

All copolymers prepared were characterized by SEC and MALDI–ToF MS, as well as ¹H NMR and ¹³C NMR spectroscopy. For SEC measurements, the samples had to be dissolved in THF for 1 day to ensure complete solubility. The resulting molecular weights and PDIs of all samples obtained by SEC (measured in THF, PS standard) as well as the comonomer fractions (vide infra) by NMR are listed in Table 1. Molecular weights range from 5100 to 31900 g·mol⁻¹ with low to moderate polydispersity (PDI) in comparison to comparable literature.^{9,46–48} SEC elugrams with varied CEO monomer ratio (from 3.3 to 29.3% of CEO incorporation in the copolymer) are shown in Figure 1. With increasing CEO

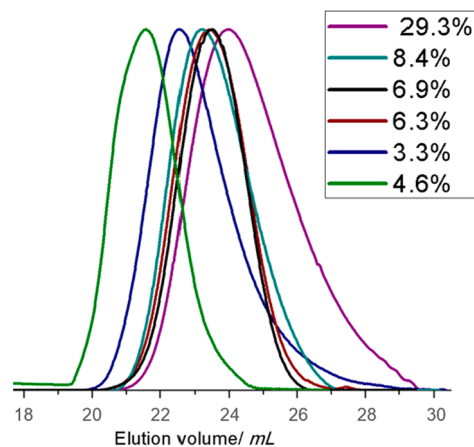


Figure 1. SEC elugrams (in THF, PS standard) of several poly(THF-*co*-CEO) copolymers with varied CEO incorporation ratio (from 3.3 to 29.3%).

fraction molecular weights clearly decrease, whereas the PDI remains unchanged. We attribute this to the coexistence of the ACE and AM mechanism. Hence, with increasing THF ratio the ACE mechanism occurs, in accordance to literature,^{24,37,38} and with increasing CEO fraction coexistence of ACE and AM mechanism seems to take place, as expected.^{24,40}

Figure 2 depicts a series of ¹H NMR spectra of copolymers with different monomer content, ranging from 3.3 to 29.3 mol % CEO. With increasing amount of CEO in the copolymers, the solubility of the materials in organic solvents decreased. Thus, in this work we aimed at materials with a minority

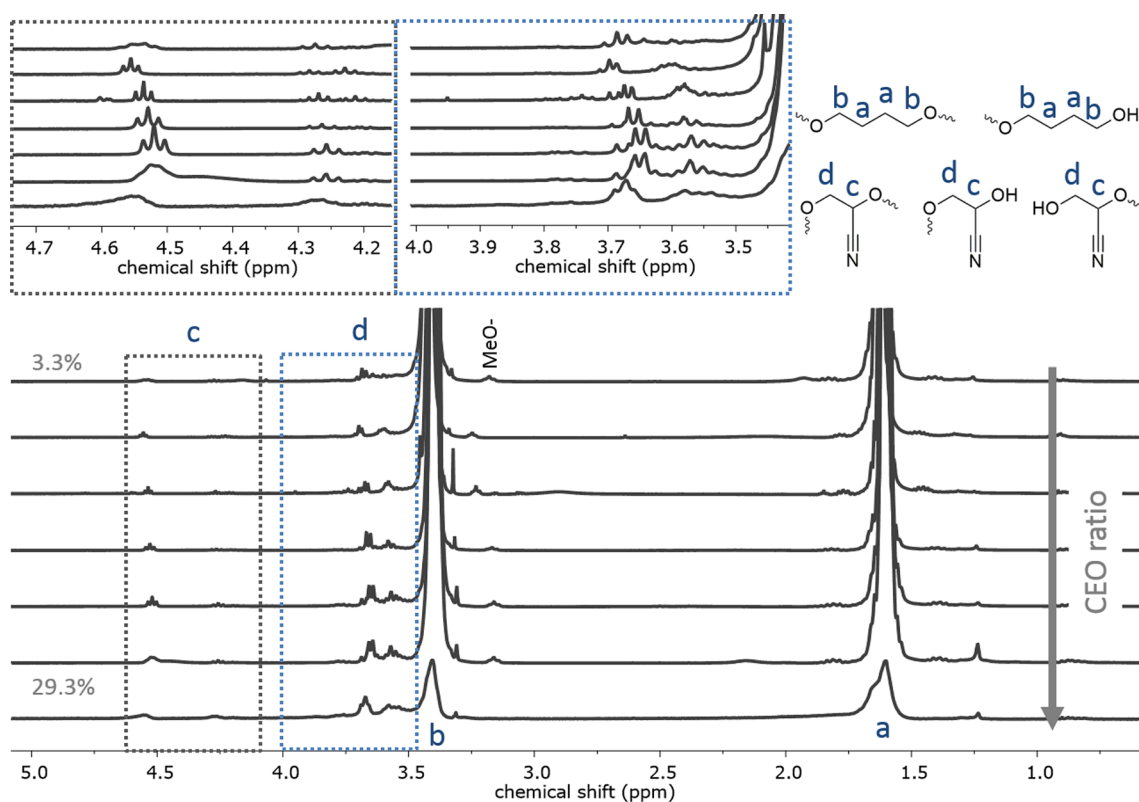


Figure 2. ^1H NMR spectra (CDCl_3 , 300 MHz) of several poly(THF-*co*-CEO) copolymers with varied monomer ratio (from 3.3 to 29.3%). Bottom: magnification of the relevant signals c and d.

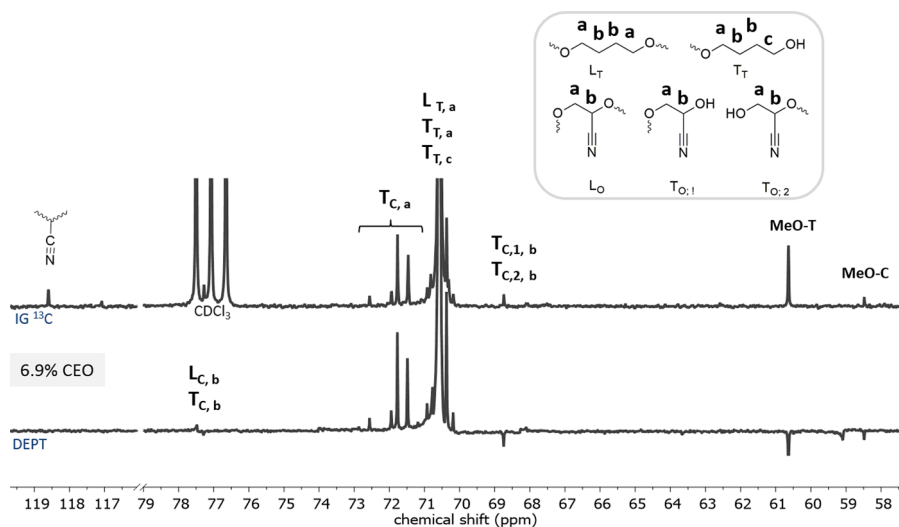


Figure 3. Top: Inverse gated ^{13}C NMR spectra (CDCl_3 , 100.6 MHz). Bottom: ^{13}C DEPT NMR spectra of P(THF-*co*-CEO) with a fraction of 6.9% CEO (CDCl_3 , 100.6 MHz) (C, CEO; T, THF).

fraction of CEO units. In the ^1H NMR spectra, the signals of the polyether backbone belonging to THF units appears at 1.47–1.74 ppm (Figure 2, a) and 3.31–3.52 ppm (Figure 2, b). The signals of the polyether backbone that stem from the CEO units are visible in the range of 4.14–4.66 ppm (Figure 2, CH) and 3.5–3.85 ppm (Figure 2, CH_2). On the basis of these assignments, the monomer incorporation rates of both THF and CEO were calculated, as listed in Table 1.

All relevant signals are found in the ^{13}C NMR spectra as well (Figure S23). Here, the signals of the polyether backbone belonging to the THF units appears at 25.25–28.04 ppm

(Figure 23, a) and 69.85–71.10 ppm (Figure S23, b). The signals of CEO units are visible at 119.75–115.7 ppm (Figure S23, CN, blue framed), 73.27–71.10 ppm (Figure S23, CH_2 , marked green) and 69.52–67.35 ppm (Figure S23, CH, marked red).

A detailed assignment of the signals in the ^{13}C NMR spectrum is shown in Figure 3 for the spectrum of the copolymer with 6.9% CEO incorporation. The assignments are supported by the results of the ^{13}C DEPT NMR (Figure 3) and are in good agreement with literature values for THF copolymers.^{43,47}

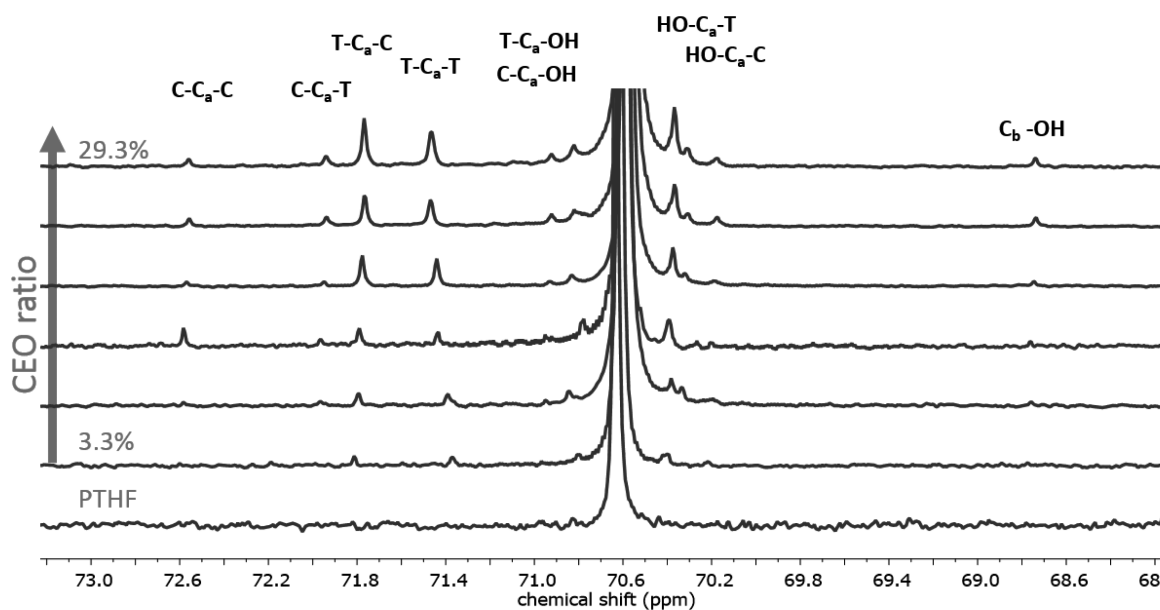


Figure 4. Relevant section of inverse gated (IG) ^{13}C NMR spectra (CDCl_3 , 100.6 MHz) of several poly(THF-co-CEO) copolymers with varied monomer ratio from 3.3 to 29.3% CEO incorporation (C, CEO; T, THF).

^{13}C NMR Triad Analysis. To gain a deeper understanding of the microstructure of the poly(THF-co-CEO) copolymers, ^{13}C NMR spectroscopy based triad analysis was carried out. The analyzed triads (i.e., sequences of three subsequent monomer units) were labeled as recently described for EO/EPICH copolymers⁴⁸ and as established for EO/PO copolymers,^{50,51} EO/DEGA copolymers¹⁷ or other amine-functional PEGs.¹⁸ Peak assignment was achieved by comparison with amine-functional PEGs^{13,18,17,52} recently synthesized in our group, as well as by comparison with THF/glycidol copolymers^{23,53} and other comparable spectra.⁴⁹ Figure 4 shows the relevant region of the *inverse gated* ^{13}C NMR spectra of several poly(THF-co-CEO) copolymers with varied CEO ratio (from 3.3 to 29.3% CEO incorporation).

With decreasing CEO content, the appropriate signals belonging to CEO at 72.58, 71.94, 72.77, 71.43, 70.93, 70.82, 70.36, 70.17, and 68.73 ppm disappear, while the CH_2 signal at 70.74–70.52 ppm, belonging to THF, is still visible, as expected. It is conspicuous that the signal belonging to the C–C–C triad does not increase with increasing CEO content, as well as the signal for the C–C–T triad. Furthermore, the triads T–C–C and T–C–T increase with increasing CEO content. We attribute this to a random or very slight gradient type microstructure, however, clearly not as a block-like structure. Besides the triad analysis of CEO units, a triad analysis of THF units was carried out as well, giving comparable results, as shown in the [Supporting Information](#) (Figure S.21).

Kinetic Studies via NMR Spectroscopy. To support the results of the triad analysis, kinetic studies have also been carried out. Different comonomer reactivity can lead to gradient type or block-like polymer chain structures, which determine the properties of the resulting materials. Hence, it is important to investigate the functional group distribution within the backbone. In the copolymerization of CEO and THF gradient copolymer structures might be expected due to the higher reactivity of oxiranes compared to oxolanes based on the respective ring strain. ^1H NMR kinetic studies were carried out by taking samples to compare the incorporation rates of THF and CEO in the copolymers. The (co)polymerization was

conducted in bulk under argon atmosphere with MeOTf as an initiator and at room temperature, following the procedure of the synthesis of the materials listed in [Table 1](#). Figure 5 shows the ^1H NMR spectrum of a mixture of CEO and THF (1:5) before initiation and several ^1H NMR spectra after initiation in a time frame of 1 min to 58 h. The kinetic studies were carried out for 58 h due to the fact that the reaction mixture had still not solidified. Compared to the synthesis of the copolymers listed in [Table 1](#) we expected solidification of the reaction mixture after 12 h. Hence, sampling of the reaction mixture seemed to impede the (co)polymerization process. However, the results show that the intensities of the signals of both monomers, CEO (3.08–2.92 ppm, green, a) and THF (1.8–1.68 ppm, blue, d), clearly decrease and signals belonging to the polymer backbone increase with increasing time. The signals of the $\text{CH}_2\text{--O--}$ groups of the backbone overlay with a signal of CEO (3.33–3.29 ppm, b) and are visible at 3.47–3.24 ppm. Further signals belonging to the backbone are present at 1.61–1.39 ppm for CH_2 groups of THF units (blue framed, d') and at 4.69–4.11 ppm for the CH groups of CEO units (green framed, b').

To confirm that the signals stem from the copolymers and not from degradation products of the monomer, diffusion ordered ^1H NMR spectroscopy (DOSY) of the purified copolymer was carried out. The obtained spectrum is shown in the [Supporting Information](#) (Figure S7) and exhibits signals at 4.60 and 4.24 ppm, which are in agreement with the signals, visible in [Figure 2](#) and with the signals obtained from the kinetic studies. However, the signals of the kinetic studies might be more precise and separated due to the good solubility of the growing oligomers. We attribute the presence of several signals for the CH groups to the fact that there might be different chemical shifts depending on whether the protons belong to terminal or linear units and whether CEO or THF is in the neighboring monomer unit. Finally, the signal at 4.6 ppm is visible via correlated spectroscopy (COSY) and correlates with the CH_2 signals of the CEO units at 3.69 ppm (please see [Supporting Information](#), Figure S8).

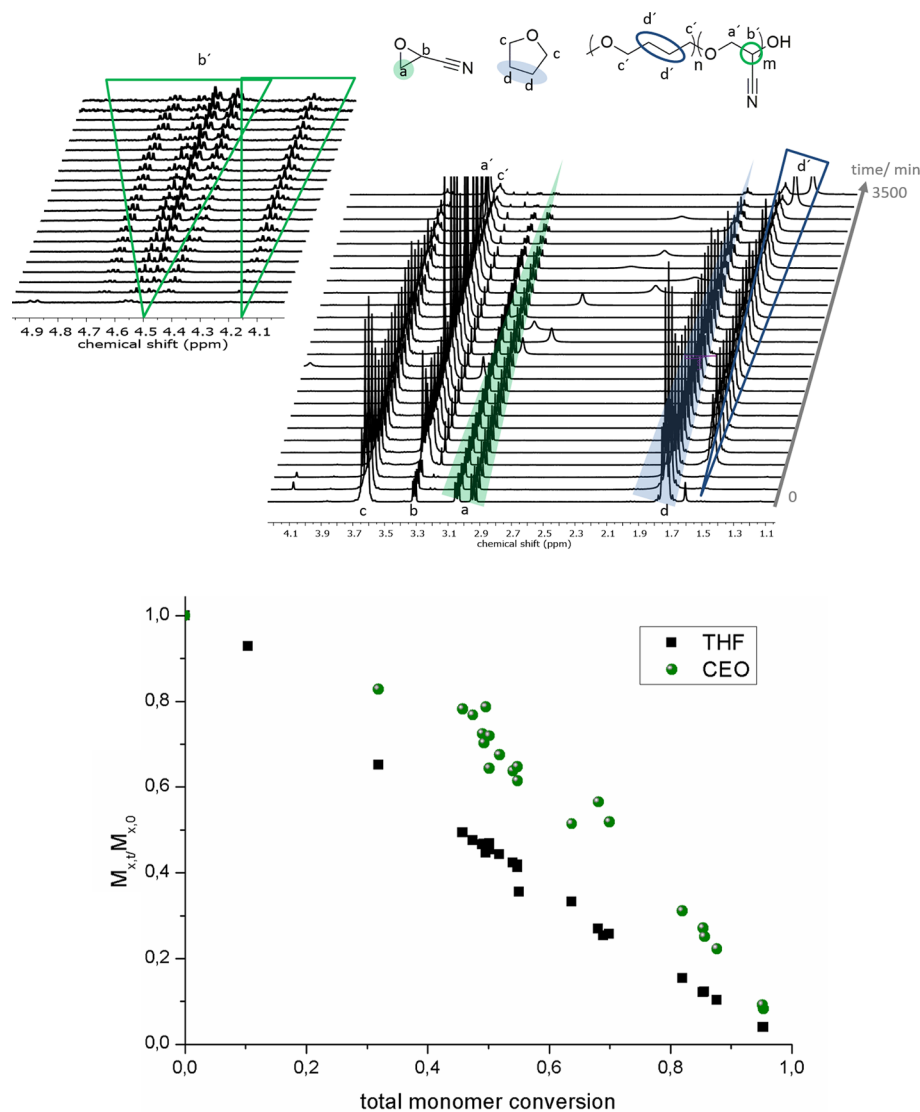


Figure 5. Kinetic studies via ^1H NMR spectroscopy (300 MHz, CDCl_3), green: CEO and blue: THF in a time frame of 1 min to 58 h, (1:5, CEO: THF), bottom: fraction of initial monomer concentration for both CEO and THF ($M_{x,t}/M_{x,0}$), normalized to 1(100%) for both monomers, respectively, vs total monomer conversion.

The results show that THF is incorporated faster than CEO (Figure 5, bottom). Thus, we expect a gradient type copolymer structure. We attribute the slower incorporation of CEO to the steric hindrance of the cyano group of the CEO comonomer, however the ring strain of oxiranes is clearly higher than for oxolanes (EO: 116 kJ mol^{-1} , THF: 23 kJ mol^{-1}).⁵⁴ Figure S3 in the Supporting Information shows a further plot of the respective monomer conversion vs total monomer conversion. In summary, the kinetic studies provide evidence for the successful incorporation of both monomers, as well as a faster incorporation of THF, leading to gradient type structures. Additionally, we conducted in situ ^1H and ^{13}C NMR kinetics in bulk, however the lack of stirring during the measurements impedes a detailed calculation of the reaction rates (Supporting Information, Figures S4–S6).

Homopolymerization of CEO was also carried out. However, as shown in the Supporting Information, the homopolymer PCEO shows very limited solubility in all solvents employed. Nevertheless, some results regarding the soluble fraction of the homopolymers are summarized in Table S3 and Figure S22 of

the Supporting Information. Molecular weights up to 2200 g mol^{-1} were detected for the soluble fraction of the homopolymers.

B. Postpolymerization Modification of Poly(THF-co-CEO) Copolymers to Water-Soluble Polyether Polyacids and Polyetheramines. Linear polyacids with tunable number of functional groups as well as molecular weights are promising for various potential applications, e.g., as gelling agents, lubricants, or ion exchange resins or for thickening in pharmaceuticals, cosmetics, and paints. The most widely applied example of polyacids is poly(acrylic acid) (PAA).⁵⁵ Especially the facile one-step postpolymerization procedure renders the novel polyTHF copolymers interesting even for potential industrial applications, due to the commercially available chemicals like sodium hydroxide and THF, as well as low temperatures ($55 \text{ }^\circ\text{C}$) and short reaction times. To date, to the best of our knowledge no postpolymerization reaction of functional polyTHF has been reported for the synthesis of linear polyacids. In order to develop water-soluble polyTHF-based polyelectrolytes, five poly(THF-co-CEO) copolymer

samples used for the generation of poly(THF-*co*-carboxylic acid ethylene oxide) (P(THF-*co*-CAEO)) have been prepared and extensively characterized by NMR, MALDI–ToF MS, and FT-IR spectroscopy.

Postpolymerization modification was carried out following the procedure of Peng et al.³¹ The poly(THF-*co*-CEO) copolymer was dissolved in THF, sodium hydroxide (1 molar) was added, and the reaction mixture was stirred overnight at 55 °C. Subsequently, the polymer was purified and the salts were removed via dialysis in THF/methanol (1:1) for 3 days. The THF/methanol mixture was renewed every 24 h. This reaction step is described in Scheme 1. All resulting polyether polyacids were soluble in water up to a concentration of 1 mg mL⁻¹ and at a pH value of 10. However, polyether polyacids with a low CAEO fraction of 3.3 and 4.6% still yield slightly cloudy solutions, which did not become clear even at higher pH values. On the other hand, regarding the insoluble polyTHF backbone of the materials it is striking that even low amounts of hydrolyzed CEO units in the copolymers lead to a certain solubility of the polyTHF copolymers in water.

Because of the known interaction of carboxylic acids with the column material, no SEC measurements were carried out for the acid functional copolymers. However, molecular weights before and after modification were comparable according to ¹H NMR. Results are listed in Table 2 and show a trend

Table 2. Characterization Data of ¹H NMR Measurements for the Series of Poly(THF-*co*-CEO) Copolymers and the Post-Polymerization Modification to P(THF-*co*-CAEO_{1-x})

CEO content ^a /%	<i>M_n</i> (NMR) ^a	
	P(THF- <i>co</i> -CEO _{1-x})	P(THF- <i>co</i> -CAEO _{1-x})
8.4	9400	12100
6.9	9100	7100
6.3	13400	10600
4.6	21800	25400
3.3	10900	9500

^aCalculated via ¹H NMR spectra in CDCl₃ (P(THF-*co*-CEO_{1-x})) and in THF-*d*₈ (P(THF-*co*-CAEO_{1-x})), 300 MHz.

concerning related molecular weights before and after postpolymerization. Some deviations occur (e.g., sample 1 in Table 2), which may be explained by utilizing different solvents for the ¹H NMR measurements (CDCl₃ for P(THF-*co*-CEO_{1-x}) and THF-*d*₈ for P(THF-*co*-CAEO_{1-x})). This was necessary to ensure well dissolved materials, given that the polyether polyacids were not completely soluble in CDCl₃, which was the preferred solvent for the poly(THF-*co*-CEO) copolymers. Most notably, results show, that the average molecular weights do not decrease, which excludes degradation of the polymer backbone during the reaction step with sodium hydroxide. We suggest a possible steric hindrance of the functional nitrile groups belonging to the CEO units, which are closer to the polyether backbone in contrast to the alkaline labile PEG-*co*-PEPICH copolymers.⁴⁸

¹H and ¹³C NMR Spectroscopy. Figure S14 depicts a series of ¹H NMR spectra of polyether polyacids with varied CEO ratio (from 3.3 to 8.4%) and a spectrum of a poly(THF-*co*-CEO) copolymer with a fraction of 3.3% CEO for comparison. At the top of Figure S14, a zoom-in of the respective spectra is shown. At 3.48–3.32 ppm and 1.56–1.54 ppm the backbone of the THF units of the copolymer is visible, which overlap with the signals of the backbone of the functionalized CEO units. The signal belonging to the CH groups of CEO units at 4.42 ppm disappears and a signal for the CH groups of the carboxylic acids after transformation appears at 5.37 ppm, demonstrating the successful postpolymerization reaction.

The successful postpolymerization modification can be shown via ¹³C NMR spectroscopy as well and even for the copolymer with a low fraction of 3.3% CEO (see Figure 6 and Figure S15). Unfortunately, it was not possible to find a solvent suitable for both copolymers before and after modification. However, the change of the solubility can be taken as a first indication for a successful postpolymerization reaction. As presented in the zoom-in in Figure 6, the signal concerning the cyanide group at 119.68–116.24 ppm disappears after conversion and a signal at 160.14 ppm appears, belonging to the carbon atoms of the carboxylic acid groups.

MALDI–ToF Mass Spectroscopy. Besides NMR spectroscopy, MALDI–ToF mass spectroscopy (MS) was performed to

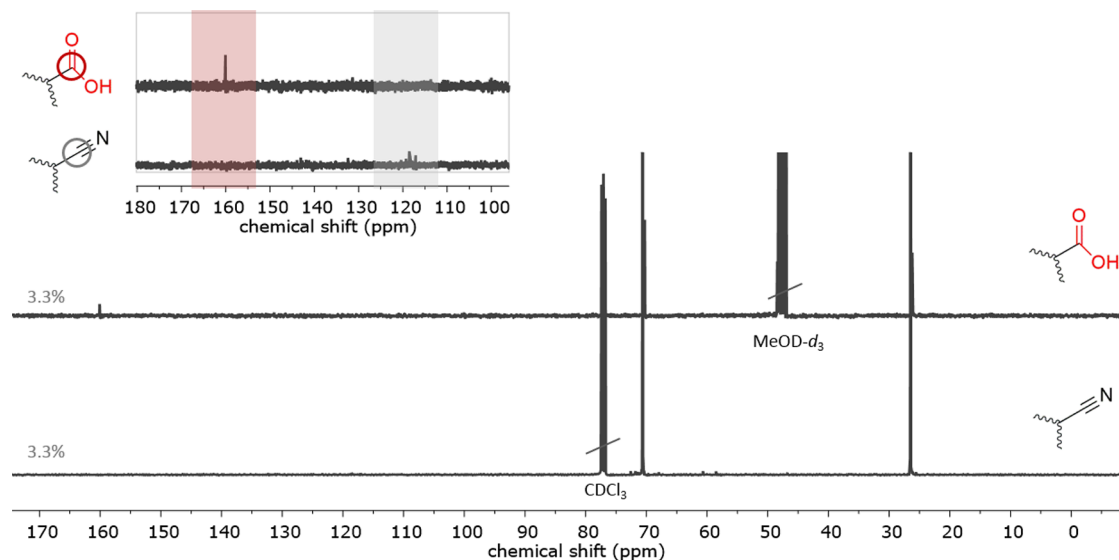


Figure 6. ¹³C NMR spectra of the CEO-THF copolymer (300 MHz, CDCl₃) with a fraction of 3.3% CEO (bottom) and the same copolymer after postpolymerization reaction to carboxylic acid groups (300 MHz, MeOD-*d*₃). Top: magnification of the relevant section.

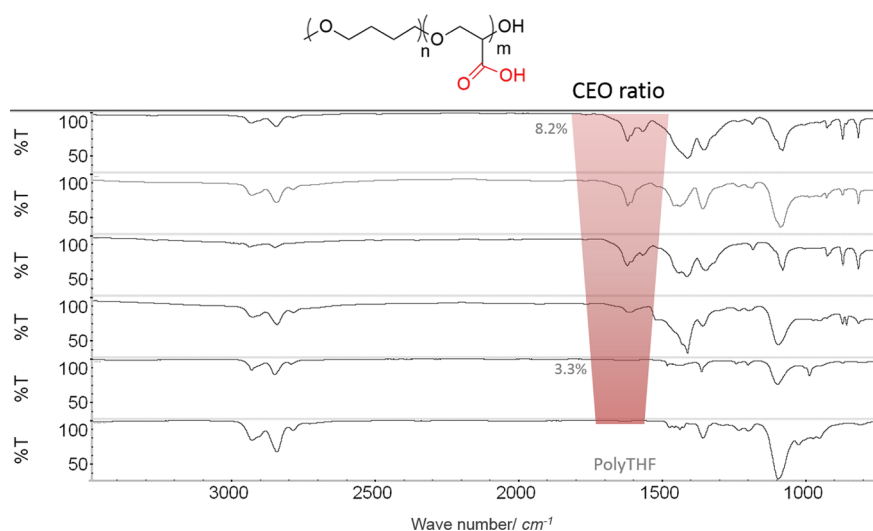


Figure 7. FT-IR spectra of several poly(THF-*co*-CAEO) copolymers with varied CEO content (3.3–8.4%) after transformation of the nitrile groups to carboxylic acid groups.

gain information on the successful copolymerization of CEO and THF, as well as to investigate the complete postpolymerization reaction of the cyanide groups. Furthermore, MALDI-ToF MS is a method to support molecular weights obtained via SEC or NMR spectroscopy, and to investigate possible degradation of the copolymers during the modification step.

Figure S9 (top) depicts the spectra of two exemplary poly(THF-*co*-CEO) copolymers with a fraction of 8.4 and 6.9% CEO, together with the spectra after postmodification to carboxylic acids of the same (blue), as well as the magnification of these spectra (bottom). A complete signal assignment is also given in Figure S9. The results show that the copolymerization of CEO and THF was successful, resulting in incorporation of both monomers. Furthermore, the postpolymerization reaction was complete, given that no residual signals of the poly(THF-*co*-CEO) copolymers were found. The average molecular weights did not vary significantly before and after postpolymerization modification (Figure S10). Molecular weights determined by MALDI-ToF were slightly smaller than observed via SEC or NMR. We attribute this to the so-called “mass discrimination effect”, which underestimates higher molecular weight fractions.^{56–58}

FT-IR Spectroscopy. As an additional method to investigate the successful copolymerization of CEO and THF, and to gather evidence for complete conversion to polyether polyacids, FT-IR spectroscopy was carried out. The normalized spectra of the five postpolymerized copolymers are depicted in Figure 7. With increasing CEO fraction, the bands at 1600–1700 cm^{-1} increase as well, which can be assigned to carboxylic salts, in accordance to literature for carboxylic acids.³¹

C. Postpolymerization Modification of Poly(THF-*co*-CEO) Copolymers: Polyetheramines. Amino-functional polyethers attract industrial as well as academic interest due to their pH-responsive behavior.^{17,18,45,48,59–61} However, not only the well-established and water-soluble poly(ethylene glycol) has been applied for this purpose. The group of Tsvetanov introduced an even more hydrophobic glycidylamine derivative, glycidyl didodecylamine to provide high solubilizing power toward extremely hydrophobic drugs.⁶²

The postpolymerization of poly(THF-*co*-CEO) copolymers to polyether polyamines permits access to amine-functionalized materials with moderate to high molecular weights. A

combination of polyTHF with functional amine groups was described in literature¹¹ with the aim to construct dendrimer containing hybrid networks.⁶³ An additional strategy to combine polyTHF with amine groups is the end-capping of polyTHF to obtain “ditopic” macromonomers.⁸ Possible applications of these structures are envisaged especially in the polyurethane (PU) production, since polyTHF is a widely used material for the soft segments in PUs and since amines are typically added to catalyze urethane formation.

Postpolymerization modification to P(THF_{*x*}-*co*-CAmEO_{1-*x*}) was carried out following the hydrogenation procedure developed by Meijer et al. for polyamine dendrimers³² and recently published routes of our group.⁴⁸ The poly(THF-*co*-CEO) copolymer was dissolved in THF, the Raney cobalt catalyst, dissolved in water, was added and the mixture was stirred under H₂ pressure for 7 days. A detailed description is given in the **experimental** section and the transformation is shown in Scheme 1. Molecular weight before and after the transformation determined via ¹H NMR is comparable as well. The results are listed in Table 3 and show similar molecular

Table 3. Characterization Data from ¹H NMR Measurements for the Series of Poly(THF-*co*-CEO) Copolymers and the Modification to P(THF_{*x*}-*co*-CAmEO_{1-*x*})

CEO content ^a /%	$M_n(\text{NMR}/\text{g}\cdot\text{mol}^{-1})^a$	
	P(THF _{<i>x</i>} - <i>co</i> -CEO _{1-<i>x</i>})	P(THF _{<i>x</i>} - <i>co</i> -CAmEO _{1-<i>x</i>})
8.4	9400	9000
6.9	9100	7700
6.3	13400	8700
4.6	21800	9600
3.3	10900	10400

^aCalculated via ¹H NMR spectra in CDCl₃, 300 MHz.

weights before and after modification, with the exception of the sample with 4.6% CEO fraction. Here, the molecular weight after postmodification is lower after hydrogenation, which attribute this to solubilizing effects of the amine groups in the solvent.

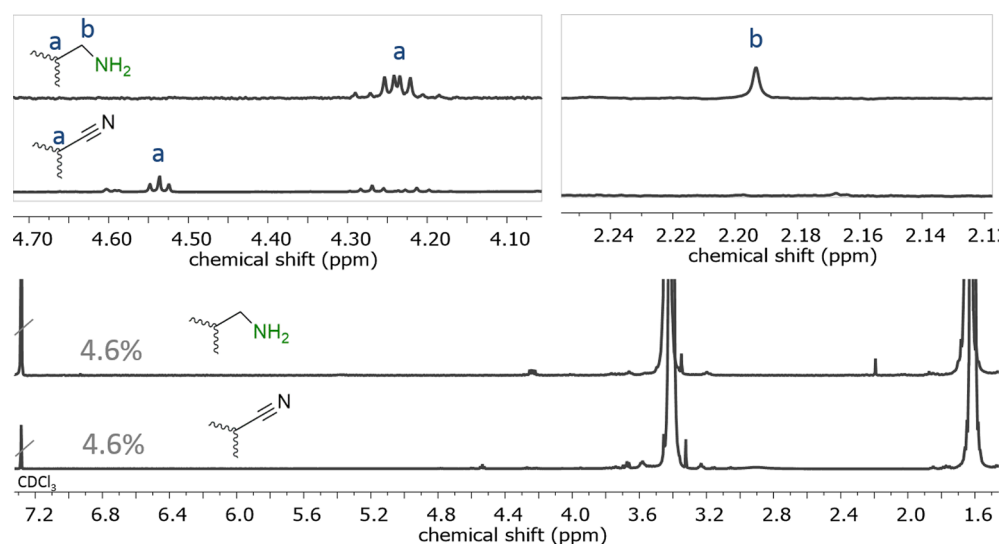


Figure 8. ^1H NMR (300 MHz, CDCl_3) of $\text{P}(\text{THF}_{0.95}\text{-co-CAmEO}_{0.05})$ (top) and the poly(THF-co-CEO) copolymer with a fraction of 4.6% CEO (bottom) and the magnification of the relevant signals, respectively.

^1H NMR Spectroscopy. Figure 8 shows the ^1H NMR spectra of the amine-functional polyTHF copolymers, together with a magnification of the relevant sections, of $\text{P}(\text{THF}_{0.95}\text{-co-CAmEO}_{0.05})$ (top) and of the poly(THF-co-CEO) copolymer with a fraction of 4.6% CEO (bottom), respectively. A detailed assignment of the signals stemming from the polymer backbone of poly(THF-co-CEO) copolymers was given in the context of the kinetic studies (Figure 5) and is comparable to the signal of the backbone of the postmodified copolymers. A clear transformation of the signals before and after postmodification is visible and depicted in the magnifications. The signal assigned to the CH groups at 4.54 ppm disappears completely and a new signal occurs at 4.26–4.21 ppm (Figure 8, top, on the left, a). Furthermore, a signal at 2.19 ppm appears, which can be assigned to the CH_2 groups next to the nitrogen atom. The chemical shift of this signal is in analogy to comparable structures in literature.^{45,48}

It is interesting to note that above a concentration of 7 mg mL^{-1} of the amine-functionalized copolymers in suitable solvents gelation is observed. Suitable solvents for the formation of organogels are all solvents that dissolve the THF units in the backbone, as listed in the Supporting Information (Table S1). The copolymers can be redissolved after drying of the gels and used for the generation of organogels again reversibly. Further work on the nature of gelation in these materials is in progress. Unfortunately, this effect impedes ^{13}C NMR measurements, due to a higher attended amount of the material in comparison to ^1H NMR measurements. However, the successful postmodification of the CEO-THF copolymers to amine groups was confirmed via MALDI-ToF MS as well as with FT-IR spectroscopy.

Via MALDI-ToF MS the transformation of the cyanide groups to amine groups was investigated. Figure S12 in the Supporting Information presents the spectrum of the exemplary poly(THF-co-CEO) copolymer, modified to amine groups, with a fraction of 8.4% CEO. No residual signals for unmodified polymer chains were founded, as can be seen after overlaying both spectra (see Figure S13). Besides MALDI-ToF MS, FT-IR spectroscopy was carried out to investigate the formation of amine groups (Figures S17). Typical for amine groups two bands at 1603.41 and

1519.3 cm^{-1} appear, which can be assigned to primary amines.⁶⁴ At 1003.91 cm^{-1} the C–N stretch is visible, followed by the “out-of-plane NH bend” at 858.65 cm^{-1} .^{64,65} The results confirm the successful transformation of the cyanide groups to carboxylic acid and amine groups, respectively.

D. Properties of the Polyether Copolymers. Differential scanning calorimetry (DSC) has been used to quantify the thermal properties of the materials. Table S2 lists the resulting melting points (T_m) of the poly(THF-co-CEO) copolymers with CEO fractions from 3.3 to 8.4%, as well as of the copolymers after postmodification to carboxylic acid and amine groups, respectively. With increasing amount of CEO in the copolymers the melting points decreased slightly from 30 (3.3% CEO) to 21 $^\circ\text{C}$ (8.4% CEO). The same trend can be seen for the carboxylic acid containing polymers, where the melting point decreased from 26 to 18 $^\circ\text{C}$ and for the amine containing polymers, where the melting point decreases from 28 to 23 $^\circ\text{C}$ (3.3 to 6.9% CEO). The melting points of the copolymers with carboxylic acid groups are slightly lower than before postmodification and lower than the melting points of the amine functionalized analogues (see Figure S18). This is in accordance with literature on related systems.⁴⁸ In one case no melting point of the amine functionalized copolymers could be obtained. This might be attributed to the functional amine groups, which seem to impede crystallization of the material. For the polyTHF homopolymer T_g values can be found in some publications and vary between -65 ⁴⁶ and -84 $^\circ\text{C}$.⁶⁶

Contact Angle Measurements. Besides the investigation of the thermal behavior, contact angle measurements of water on $\text{P}(\text{THF-co-CEO})$ -films have been carried out to assess surface properties of the materials. Furthermore, contact angles on films of $\text{P}(\text{THF-co-CEO})$ as well as $\text{P}(\text{THF-co-CEAmO})$ were measured to investigate the different surface tensions of these materials, before and after postmodification. As expected, with decreasing CEO content in the copolymers, the materials showed increasing solubility in hydrophobic solvents. After postmodification, the carboxylic acid groups in the copolymer should contribute to lowered contact angles. Figure 9 shows the measured contact angles for the copolymers (Figure 9, black: $\text{P}(\text{THF-co-CEO})$, green: $\text{P}(\text{CEAmO-co-THF})$, red: $\text{P}(\text{CEAO-co-THF})$). Silicon wafers were coated using copolymer

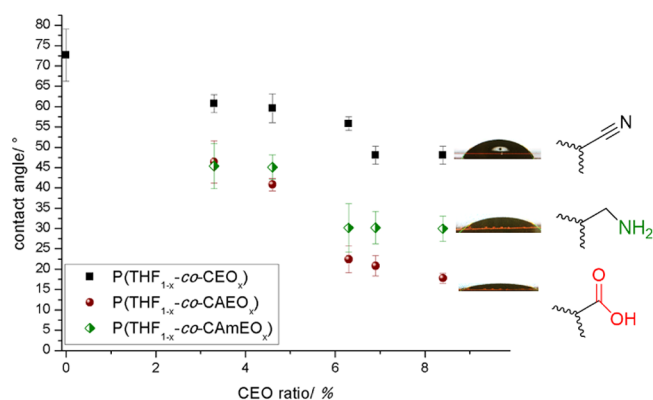


Figure 9. Contact angles of water at P(CEO_x-co-THF_{1-x})-films at different CEO/THF ratios (black), as well as contact angles of water on postmodified copolymer-films to carboxylic acids (red) and amines (green).

solutions in chloroform or THF. Subsequently, the solvent was evaporated under reduced pressure at 90 °C for 24 h. With increasing amount of CEO the contact angle decreased from 60.7° for 3.3% CEO units down to 48.0° for 8.4% CEO units. For the apolar polyTHF, we obtained a contact angle of 72.7°. The results mirror the content of CEO, as expected. After postmodification, contact angles decrease slightly for the carboxylic acids as well as for the amines, however the effect is more pronounced for the carboxylic acids. For instance, for the copolymer with 8.4% carboxylic acid groups the contact angle decreases to 17.8°, reflecting a highly polar film surface. With regard to the high contact angle of polyTHF (72.7°), even the low content of 8.4% carboxylic acid groups in the materials shows a strong effect on the contact angles.

E. Mineralization of Calcium Carbonate. To the best of our knowledge, polyethers with carboxylic acids have not been employed for mineralization experiments, mainly due to their very limited availability. In the case of the carboxylic acid functional polyTHF copolymers, the unusual combination of an apolar backbone with a controlled number of hydrophilic carboxylic acid groups is an intriguing precondition for such studies. CaCO₃ is a well-established inorganic model system for studying the effect of additives on the crystallization behavior.^{33–35,67} Besides its industrial importance as a major source of water hardness,⁶⁸ as a mineral filler^{69,70} or raw material for construction chemicals^{71,72} CaCO₃ also represents the most common biomineral with complex morphologies and crystals exhibiting defined crystallographic orientations in shells⁷³ and exoskeletons.^{74,75} A key feature of many biominerals is that they are composed of smaller crystals of similar size and shape, which are arranged in a regular periodic pattern. Cölfen and co-workers coined the term mesocrystal⁶⁷ to describe this oriented aggregation, where the smaller crystals have parallel crystallographic alignment.^{76,77} Especially for potential use as antiscalant or as soft component in a CaCO₃ hybrid material the influence of polyether polyacids on the precipitation of CaCO₃ has to be understood.⁷⁸ In this context, the postmodified carboxylic acid functional poly(THF-co-CEO) copolymers have been used as additives to crystallize CaCO₃ on quartz glass slides.

As shown in Figure 10, without any additive CaCO₃ crystallizes in its thermodynamically most stable polymorph calcite with rhombohedral crystal morphology and crystal sizes between 10 and 20 μm and terminated by the [104] facets (the

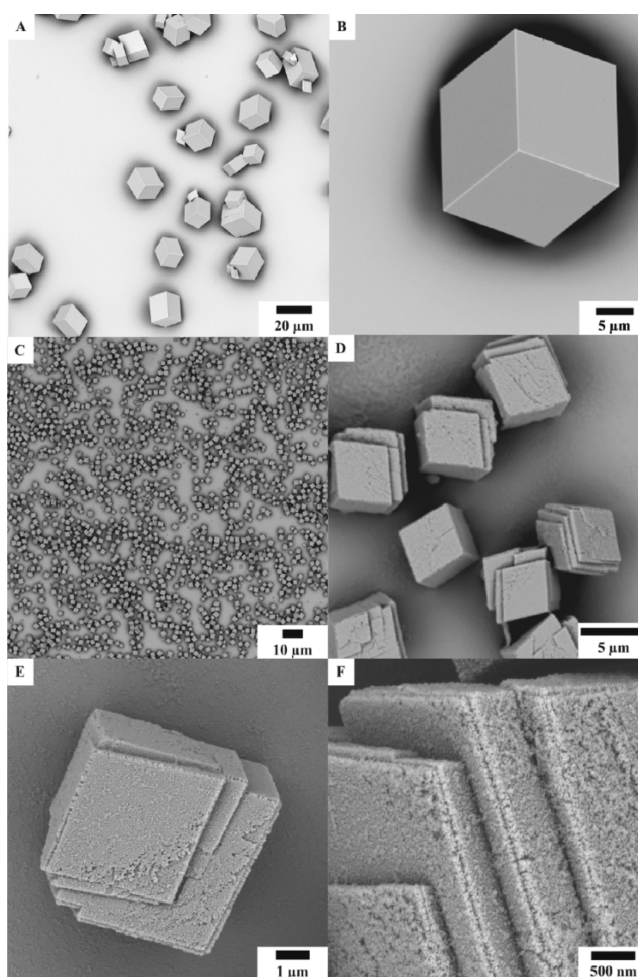


Figure 10. SEM images (A, B) calcite reference; (C–F) calcite crystals precipitated in the presence of 0.04 mmol·L⁻¹ of postmodified copolymer with a fraction of 8.4% CEO (sample 1, listed in Table 2) to polyacids.

most stable and apolar surfaces). The most pronounced effect on crystal growth is observed on facets with highest polarity. These are the [010] and [012] facets, which are oriented parallel to the spatial (*c* axis) of the rhombohedra.⁷⁹ In the presence of polar additives polar steps are formed because of a stabilization of the polar edges.⁷⁹ If this occurs extensively, the crystals will be elongated along the *c* axis,⁸⁰ as shown in the SEM images in Figure 10D–F. In addition, the decrease of the crystal size from approximately 10–20 μm to 3–5 μm through the polyether-polyacid additive (Figure 10C) indicates either (i) an increase of the nucleation density or (ii) an inhibition of the crystal growth. The model of growth inhibition is supported by a statistical evaluation of the sizes of 100 mesocrystals (Figures S19 and S20, Supporting Information) formed after adding modified copolymers with increasing amounts of CEO. A plot of the number of carboxylate groups of the polymer versus the maxima of the Gaussian trend lines (Figure S19) clearly shows a linear decrease of the CaCO₃ crystal size with the content of carboxylate groups in the PTHF copolymers. This indicates that strong surface binding of the polymer to the crystal steps through Ca²⁺ surface complexation and a concomitant increase of the number of steps (Figure S21 C,D for 3.3% of CEO and Figure 10 for 8.4% of CEO). The polar steps are stabilized to a different extent by CEO groups,

as illustrated in Scheme S1 (Supporting Information). We assume that for copolymers with a smaller amount of statistically distributed acidic groups a more flexible polymer chain is adsorbed on the polar facets. The loosely bound polymer does not provide full surface coverage, and CaCO_3 continues to precipitate, whereas an even higher amount of CEO groups forces stronger, less loopy and thus tighter binding of the polymer. This prevents ions from adsorbing on the edges, and new edges start to form. Surprisingly, the hydrophobic backbone appears to exert a stronger stabilizing effect than the acidic binding groups due to steric shielding.

The growth of calcite rhombohedra can be understood from Figure 10F showing a calcite mesocrystal with the characteristic calcite morphology composed of nanoscopic surface-functionalized building blocks. This is in agreement with the outcome of previous studies, where a polymer-induced liquid precursor phase (PILP)^{80,81} stabilized by PAA^{35,76,82–88} or Ca-binding proteins^{75,89,90} played a leading role for the formation of mesocrystals.⁶⁷

This hypothesis is also supported by TEM images (Figure 11) showing the formation of an amorphous (PILP) polymer-

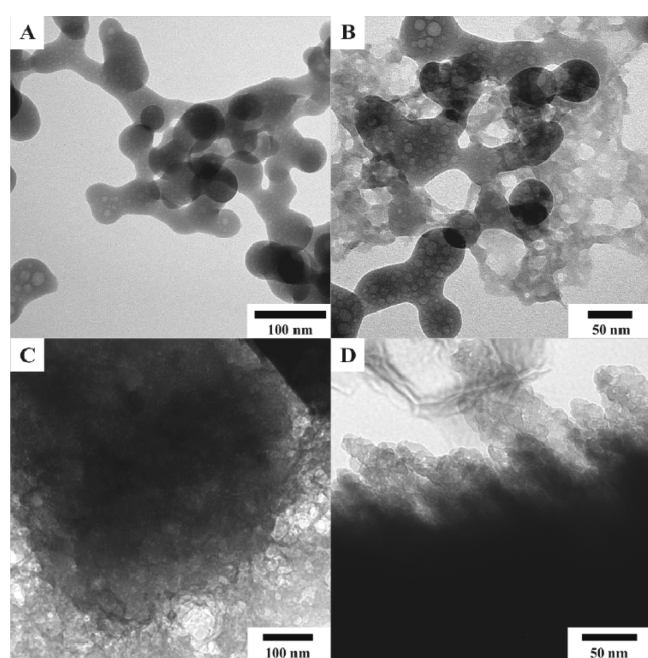


Figure 11. TEM images of polymer micelles before crystallization (A), polymer micelles and PILP after 1 h (B), agglomerated ACC from PILP after 2 h (C), microstructure of CaCO_3 particles agglomerated on calcite rhombohedra after 4 h of reaction time (D). All samples were prepared in the presence of 0.04 mmol/L of postmodified copolymer with 8.4% CEO fraction.

stabilized liquid-like phase. The solidification of the liquid droplets (Figure 11A) starts 1 h after initiating the ammonia diffusion in a desiccator (Figure 11B). Further increase of the CO_2 concentration leads to the formation of amorphous calcium carbonate (ACC) agglomerates from the PILP (Figure 11C) and CaCO_3 particles agglomerated on the surfaces of calcite rhombohedra.

The effect of the polymer is also visible in the Raman spectra (Figure S22, Supporting Information), where besides the calcite bands a background fluorescence signal of the polymer was observed. The lattice mode at 283 cm^{-1} is shifted to lower

wavenumbers (279 cm^{-1}). The broadening of all other signals indicates the presence of noncrystalline domains.^{91,92} In essence, the strong surface binding properties make polyTHF polyacids an efficient crystallization inhibitor for the precipitation of CaCO_3 (in analogy to the more polar PAA).⁸³ The strong stabilization in spite of a smaller number of acidic groups is due to steric shielding of the polar edges by the more hydrophobic backbone of polyTHF.

CONCLUSIONS

PolyTHF is generally known as an apolar, flexible polymer. In this work, we demonstrate that copolymerization of minor amounts of a novel functional epoxide can be exploited to generate new polyTHF copolymers that are water-soluble at elevated pH and can even be used for mineralization studies in aqueous solution, despite the mainly apolar polyTHF backbone structure. To date copolymers consisting of THF and functional monomer units have hardly been investigated.^{8–11} Here the random cationic ring-opening copolymerization of THF and cyano ethylene oxide (CEO) has been studied, using varied CEO fractions from 3.3 to 29.3% and molecular weights in the range of 5100 and $31900\text{ g}\cdot\text{mol}^{-1}$ (molecular weight distributions: 1.31–1.74, SEC in THF, PS standards, RI detector). The polymerization was conducted with methyl trifluoromethanesulfonate (MeOTf), and kinetic studies concerning the reactivity of both monomers have been performed via NMR spectroscopy. Furthermore, we present postmodification reactions of the cyano groups to carboxylic acid groups as well as to amine groups in a one-step procedure. The copolymerization of CEO and THF and the postmodification reactions have been characterized via NMR, MALDI–ToF mass and FT-IR spectroscopy. The thermal properties of the materials have been examined via DSC. To investigate surface properties, contact angles have been measured, which can be tuned in the range of 72.7° to 17.8° by varying the CEO fraction as well as by postmodification. The effect of polyether polyacids with different amounts of carboxylic groups on the crystallization of CaCO_3 is not only dominated by the number of carboxylate groups but also by the steric shielding of the hydrophobic polyTHF backbone. The polyether polyols seem to play multiple roles during crystallization by (i) acting as nucleation sites, (ii) stabilizing liquid droplets of amorphous CaCO_3 (PILP) and (iii) inhibiting the growth of calcite by surface binding. Further studies on the materials properties of these unusual functional polyethers are under way.

ASSOCIATED CONTENT

Supporting Information

The Supporting Information is available free of charge on the ACS Publications website at DOI: 10.1021/acs.macromol.6b00113.

Additional ^1H , ^{13}C , DOSY, NMR kinetics, MALDI–ToF and IR spectra and other characterization data (PDF)

AUTHOR INFORMATION

Corresponding Author

*(H.F.) E-mail: hfrey@uni-mainz.de.

Notes

The authors declare no competing financial interest.

ACKNOWLEDGMENTS

E.-M.C. and J.H. thank the Graduate School of Excellence Material Science in Mainz "MAINZ" for financial support and acknowledges technical assistance from Michael Bläser. J.H. is grateful to the Fonds der Chemischen Industrie for a scholarship. M.M. thanks the Max Planck Graduate Center for financial support and technical assistance. The authors thank Manfred Wagner for measuring the in situ NMR kinetics in bulk.

REFERENCES

- (1) Dreyfuss, P.; Dreyfuss, M. P. Polytetrahydrofuran. *Adv. Polym. Sci.* **1967**, *4*, 528–590.
- (2) Hwang, K. K. S.; Wu, G.; Lin, S. B.; Cooper, S. L. Cooper Synthesis and characterization of MDI-butenediol urethane model compounds. *J. Polym. Sci., Polym. Chem. Ed.* **1984**, *22*, 1677–1697.
- (3) Odarchenko, Y. I.; Sijbrandi, N. J.; Rosenthal, M.; Kimenai, A. J.; Mes, E. P. C.; Broos, R.; Bar, G.; Dijkstra, P. J.; Feijen, J.; Ivanov, D. A. Structure formation and hydrogen bonding in all-aliphatic segmented copolymers with uniform hard segments. *Acta Biomater.* **2013**, *9*, 6143–6149.
- (4) Guillaume, S. M.; Mespouille, L. Polycarbonates and green chemistry. *J. Appl. Polym. Sci.* **2014**, *131*, 40081.
- (5) Kultys, A.; Puszka, A. Transparent poly(thiourethane-urethane)s based on dithiol chain extender. *J. Therm. Anal. Calorim.* **2014**, *117*, 1427–1439.
- (6) Enthaler, S.; Trautner, A. Iron-catalyzed ring-closing depolymerization of poly(tetrahydrofuran). *ChemSusChem* **2013**, *6*, 1334–1336.
- (7) Enthaler, S. Zinc(II)-triflate as catalyst precursor for ring-closing depolymerization of end-of-life polytetrahydrofuran to produce tetrahydrofuran. *J. Appl. Polym. Sci.* **2014**, *131*, 39791.
- (8) Sivakova, S.; Bohnsack, D. A.; Mackay, M. E.; Suwanmala, P.; Rowan, S. J. Utilization of a combination of weak hydrogen-bonding interactions and phase segregation to yield highly thermosensitive supramolecular polymers. *J. Am. Chem. Soc.* **2005**, *127*, 18202–18211.
- (9) Dubreuil, M. F.; Farcy, N. G.; Goethals, E. J. Influence of the alkyl group of triflate esters on their initiation ability for the cationic ring-opening polymerization of tetrahydrofuran. *Macromol. Rapid Commun.* **1999**, *20*, 383–386.
- (10) Lim, S.-H.; Cha, E.-J.; Huh, J.; Ahn, C.-H. Micelle Behavior of Copolymers Composed of Linear and Hyperbranched Blocks in Aqueous Solution. *Macromol. Chem. Phys.* **2009**, *210*, 1734–1738.
- (11) Tanghe, L. M.; Goethals, E. J.; Du Prez, F. Segmented polymer networks containing amino-dendrimers. *Polym. Int.* **2003**, *52*, 191–197.
- (12) Liu, Y.; Huang, K.; Peng, D.; Wu, H. Synthesis, characterization and hydrolysis of an aliphatic polycarbonate by terpolymerization of carbon dioxide, propylene oxide and maleic anhydride. *Polymer* **2006**, *47*, 8453–8461.
- (13) Obermeier, B.; Wurm, F.; Frey, H. Amino Functional Poly(ethylene glycol) Copolymers via Protected Amino Glycidol. *Macromolecules* **2010**, *43*, 2244–2251.
- (14) Brocas, A.-L.; Mantzaridis, C.; Tunc, D.; Carlotti, S. Polyether synthesis: From activated or metal-free anionic ring-opening polymerization of epoxides to functionalization. *Prog. Polym. Sci.* **2013**, *38*, 845–873.
- (15) Mangold, C.; Wurm, F.; Frey, H. Functional PEG-based polymers with reactive groups via anionic ROP of tailor-made epoxides. *Polym. Chem.* **2012**, *3*, 1714.
- (16) Ye, L.; Feng, Z.-g.; Su, Y.-f.; Wu, F.; Chen, S.; Wang, G.-q. Synthesis and characterization of homo- and copolymers of 3-(2-cyanoethoxy)methyl- and 3-[methoxy(triethylenoxy)]methyl-3'-methyl-oxetane. *Polym. Int.* **2005**, *54*, 1440–1448.
- (17) Reuss, V. S.; Werre, M.; Frey, H. Thermoresponsive copolymers of ethylene oxide and N,N-diethyl glycidyl amine: polyether polyelectrolytes and PEGylated gold nanoparticle formation. *Macromol. Rapid Commun.* **2012**, *33*, 1556–1561.
- (18) Herzberger, J.; Kurzbach, D.; Werre, M.; Fischer, K.; Hinderberger, D.; Frey, H. Stimuli-Responsive Tertiary Amine Functional PEGs Based on N,N-Dialkylglycidylamines. *Macromolecules* **2014**, *47*, 7679–7690.
- (19) Shintani, Y.; Tsutsumi, H. Ionic conducting behavior of solvent-free polymer electrolytes prepared from oxetane derivative with nitrile group. *J. Power Sources* **2010**, *195*, 2863–2869.
- (20) Cohen, P.; Abadie, M.; Schué, F.; Richards, D. H. Reaction of living polyTHF with amines: 4. Primary amines. *Polymer* **1982**, *23*, 1350–1354.
- (21) Rajendran, G. P.; Mahadevan, V.; Srinivasan, M. Synthesis of some low glass transition temperature polytetrahydrofuran polymers. *Eur. Polym. J.* **1989**, *25*, 461–463.
- (22) Tarrés, M.; Viñas, C.; Cioran, A. M.; Hänninen, M. M.; Sillanpää, R.; Teixidor, F. Towards multifunctional materials incorporating elastomers and reversible redox-active fragments. *Chem. - Eur. J.* **2014**, *20*, 15808–15815.
- (23) Bednarek, M.; Kubisa, P. Cationic copolymerization of tetrahydrofuran with ethylene oxide in the presence of diols. *J. Polym. Sci., Part A: Polym. Chem.* **1999**, *37* (17), 3455–3463.
- (24) Hövetborn, T.; Hölscher, M.; Keul, H.; Höcker, H. poly(ethylene oxide-co-tetrahydrofuran) and poly(propylene oxide-co-tetrahydrofuran): Synthesis and Thermal Degradation. *Rev. Roum. Chim.* **2006**, *7–8*, 781–793.
- (25) Fan, W.-w.; Fan, X.-d.; Tian, W.; Zhang, X.; Wang, G.; Zhang, W.-b.; Bai, Y.; Zhu, X.-z. Phase transition dynamics and mechanism for backbone-thermo-responsive hyperbranched polyethers. *Polym. Chem.* **2014**, *5*, 4022.
- (26) Rubio-Cervilla, J.; Barroso-Bujans, F.; Pomposo, J. A. Merging of Zwitterionic ROP and Photoactivated Thiol–Yne Coupling for the Synthesis of Polyether Single-Chain Nanoparticles. *Macromolecules* **2016**, *49*, 90–97.
- (27) Basko, M.; Bednarek, M.; Billiet, L.; Kubisa, P.; Goethals, E.; Du Prez, F. J. Combining cationic ring-opening polymerization and click chemistry for the design of functionalized polyurethanes. *J. Polym. Sci., Part A: Polym. Chem.* **2011**, *49*, 1597–1604.
- (28) Mohan, Y. M.; Raju, K. M. Synthesis and Characterization of GAP-THF Copolymers. *Int. J. Polym. Mater.* **2006**, *55*, 203–217.
- (29) Penczek, I.; Penczek, S. Tetrahydrofuran–3,3-bis-(chloromethyl)-oxetane copolymerization catalyzed by (i-Bu)3Al. *J. Polym. Sci., Part B: Polym. Lett.* **1967**, *5*, 367–373.
- (30) Kopecký, J.; Šmejkal, J. Einfache Darstellung von Acrylnitrilmataboliten: Oxirancarbnitril und 2,3-Dihydroxy-propionitril. *Z. Chem.* **1984**, *24*, 211–212.
- (31) Zhang, S.; Du, J.; Sun, R.; Li, X.; Yang, D.; Zhang, S.; Xiong, C.; Peng, Y. Synthesis of heterobifunctional poly(ethylene glycol) with a primary amino group at one end and a carboxylate group at the other end. *React. Funct. Polym.* **2003**, *56*, 17–25.
- (32) de Brabander-van den Berg, E. M. M.; Meijer, E. W. Poly(propylene imine) Dendrimers: Large-Scale Synthesis by Heterogeneously Catalyzed Hydrogenations. *Angew. Chem., Int. Ed. Engl.* **1993**, *32*, 1308–1311.
- (33) Küther, J.; Seshadri, R.; Knoll, W.; Tremel, W. Templated growth of calcite, vaterite and aragonite crystals on self-assembled monolayers of substituted alkythiols on gold. *J. Mater. Chem.* **1998**, *8*, 641–650.
- (34) Küther, J.; Seshadri, R.; Tremel, W. Crystallization of Calcite Spherules around Designer Nuclei. *Angew. Chem., Int. Ed.* **1998**, *37*, 3044–3047.
- (35) Gebauer, D.; Cölfen, H.; Verch, A.; Antonietti, M. The Multiple Roles of Additives in CaCO₃ Crystallization: A Quantitative Case Study. *Adv. Mater.* **2009**, *21*, 435–439.
- (36) Wei, P. E.; Butler, P. E. *J. Polym. Sci., Part A-1: Polym. Chem.* **1968**, *6*, 2461–2475.
- (37) Guo, A.-r.; Yang, F.; Yu, R.; Wu, Y.-x. Real-time monitoring of living cationic ring-opening polymerization of THF and direct prediction of equilibrium molecular weight of polyTHF. *Chin. J. Polym. Sci.* **2015**, *33*, 23–35.

- (38) Kobayashi, S.; Danda, H.; Saegusa, T. Superacids and Their Derivatives. IV. Kinetic Studies on the Ring-Opening Polymerization of Tetrahydrofuran Initiated with Ethyl Trifluoromethanesulfonate by Means of ^{19}F and ^1H Nuclear Magnetic Resonance Spectroscopy. Evidence for the Oxonium-Ester Equilibrium of the Propagating Species. *Macromolecules* **1974**, *7*, 415–420.
- (39) Alder, R. W.; Phillips, J. G. E.; Huang, L.; Huang, X. Methyltrifluoromethanesulfonate. *e-EROS Encyclopedia of Reagents for Organic Synthesis* **2005**, *1*.
- (40) Asenjo-Sanz, I.; Veloso, A.; Miranda, J. I.; Alegria, A.; Pomposo, J. A.; Barroso-Bujans, F. Zwitterionic Ring-Opening Copolymerization of Tetrahydrofuran and Glycidyl Phenyl Ether with $\text{B}(\text{C}_6\text{F}_5)_3$. *Macromolecules* **2015**, *48*, 1664–1672.
- (41) Kubisa, P. *Polymer Science: A Comprehensive Reference*; Penczek, S., Grubbs, R. H., Eds.; Elsevier: Amsterdam, 2012; Vol. 4, pp 141–163.
- (42) Wu, Q.; Li, L.; Yu, Y.; Tang, X. The linear relations and living feature in cationic ring-opening copolymerization of epoxy/THF system. *Colloid Polym. Sci.* **2008**, *286*, 761–767.
- (43) Vandenberg, E. J.; Mullis, J. C. Coordination copolymerization of tetrahydrofuran and oxepane with oxetanes and epoxides. *J. Polym. Sci., Part A: Polym. Chem.* **1991**, *29*, 1421–1438.
- (44) Abe, S.; Ito, M.; Namba, K. *Makromol. Chem.* **1970**, *134*, 121–127.
- (45) Meyer, J.; Keul, H.; Möller, M. Poly(glycidyl amine) and Copolymers with Glycidol and Glycidyl Amine Repeating Units: Synthesis and Characterization. *Macromolecules* **2011**, *44*, 4082–4091.
- (46) Schüll, C.; Rabbel, H.; Schmid, F.; Frey, H. Polydispersity and Molecular Weight Distribution of Hyperbranched Graft Copolymers via “Hypergrafting” of ABm Monomers from Polydisperse Macroinitiator Cores: Theory Meets Synthesis. *Macromolecules* **2013**, *46*, 5823–5830.
- (47) Van Caeter, P.; Goethals, E. J.; Gancheva, V.; Velichkova, R. Synthesis and bulk properties of poly(tetrahydrofuran)-poly(2-methyl-2-oxazoline) ABA triblock copolymers. *Polym. Bull.* **1997**, *39*, 589–596.
- (48) Herzberger, J.; Frey, H. Epicyanohydrin: Polymerization by Monomer Activation Gives Access to Nitrile-, Amino-, and Carboxyl-Functional Poly(ethylene glycol). *Macromolecules* **2015**, *48*, 8144.
- (49) Wilms, D.; Schömer, M.; Wurm, F.; Hermanns, M. I.; Kirkpatrick, C. J.; Frey, H. Hyperbranched PEG by random copolymerization of ethylene oxide and glycidol. *Macromol. Rapid Commun.* **2010**, *31*, 1811–1815.
- (50) Hamaide, T.; Goux, A.; Llauro, M.-F.; Spitz, R.; Guyot, A. Statpoly(ethylene oxide-co-propylene oxide). *Angew. Makromol. Chem.* **1996**, *237*, 55–77.
- (51) Rejsek, V.; Sauvanier, D.; Billouard, C.; Desbois, P.; Deffieux, A.; Carloti, S. Controlled Anionic Homo- and Copolymerization of Ethylene Oxide and Propylene Oxide by Monomer Activation. *Macromolecules* **2007**, *40*, 6510–6514.
- (52) Reuss, V. S.; Obermeier, B.; Dingels, C.; Frey, H. N,N-Diallylglycidylamine: A Key Monomer for Amino-Functional Poly(ethylene glycol) Architectures. *Macromolecules* **2012**, *45*, 4581–4589.
- (53) Fan, W.-w.; Fan, X.-d.; Tian, W.; Zhang, X.; Wang, G.; Zhang, W.-b.; Bai, Y.; Zhu, X.-z. Phase transition dynamics and mechanism for backbone-thermoreponsive hyperbranched polyethers. *Polym. Chem.* **2014**, *5*, 4022.
- (54) Dreyfuss, P. *Poly(tetrahydrofuran)*, 8th ed.; Gordon and Breach, Science Publishers, Inc.: New York, 1982.
- (55) Orwoll, R. A.; Yong, C. S. *Polymer Data Handbook*; Oxford University Press, Inc.: 1999.
- (56) Schüll, C.; Nuhn, L.; Mangold, C.; Christ, E.; Zentel, R.; Frey, H. Linear-Hyperbranched Graft-Copolymers via Grafting-to Strategy Based on Hyperbranched Dendron Analogues and Reactive Ester Polymers. *Macromolecules* **2012**, *45*, 5901–5910.
- (57) Christ, E. M.; Hobernik, D.; Bros, M.; Wagner, M.; Frey, H. Cationic Copolymerization of 3,3-Bis(hydroxymethyl)oxetane and Glycidol: Biocompatible Hyperbranched Polyether Polyols with high Content of Primary Hydroxyl Groups. *Biomacromolecules* **2015**, *16*, 3297–3307.
- (58) Magnusson, H.; Malmström, E.; Hult, A. Synthesis of hyperbranched aliphatic polyethers via cationic ring-opening polymerization of 3-ethyl-3-(hydroxymethyl)oxetane. *Macromol. Rapid Commun.* **1999**, *20*, 453–457.
- (59) Wilms, V. S.; Frey, H. Aminofunctional polyethers: smart materials for applications in solution and on surfaces. *Polym. Int.* **2013**, *62*, 849–859.
- (60) Kurzbach, D.; Wilms, V. S.; Frey, H.; Hinderberger, D. Impact of Amino-Functionalization on the Response of Poly(ethylene glycol) (PEG) to External Stimuli. *ACS Macro Lett.* **2013**, *2*, 128–131.
- (61) Isono, T.; Asai, S.; Satoh, Y.; Takaoka, T.; Tajima, K.; Kakuchi, T.; Satoh, T. Controlled/Living Ring-Opening Polymerization of Glycidylamine Derivatives Using t-Bu-P 4 /Alcohol Initiating System Leading to Polyethers with Pendant Primary, Secondary, and Tertiary Amino Groups. *Macromolecules* **2015**, *48*, 3217–3229.
- (62) Rangelov, S.; Tsvetanov, C. Towards the synthesis of amino-substituted epoxides: synthesis and characterization of glycidyl-dodecylamine. *Des. Monomers Polym.* **2001**, *4* (1), 39–43.
- (63) Tanghe, L. M.; Goethals, E. J. *e-Polym.* **2001**, *1*, 017.
- (64) Smith, B. *Infrared Spectral Interpretation. A Systematic Approach*; CRC Press LLC: USA, 1999.
- (65) Génin, F.; Quilès, F.; Burneau, A. Infrared and Raman spectroscopic study of carboxylic acids in heavy water. *Phys. Chem. Chem. Phys.* **2001**, *3*, 932–942.
- (66) Gaur, U.; Wunderlich, B. Heat Capacity and Other Thermodynamic Properties of Linear Macromolecules. *J. Phys. Chem. Ref. Data* **1981**, *10*, 1001–1049.
- (67) Cölfen, H.; Antonietti, M. *Mesocrystals and Nonclassical Crystallization*; John Wiley & Sons Ltd: Chichester, England, 2008.
- (68) Schade, G. Water-dispersible ester resin containing a moiety of polyacid or bivalent alcohol containing a sulfo group. US 4,104,262, 1976.
- (69) Zuiderduin, W.; Westzaan, C.; Huétink, J.; Gaymans, R. Toughening of polypropylene with calcium carbonate particles. *Polymer* **2003**, *44*, 261–275.
- (70) Mihai, M.; Schwarz, S.; Doroftei, F.; Simionescu, B. C. Calcium Carbonate/Polymers Microparticles Tuned by Complementary Polyelectrolytes as Complex Macromolecular Templates. *Cryst. Growth Des.* **2014**, *14*, 6073–6083.
- (71) Rieger, J.; Kellermeier, M.; Nicoleau, L. Die Bildung von Nanopartikeln und Nanostrukturen - CaCO_3 , Zement und Polymere aus Sicht der Industrie. *Angew. Chem., Int. Ed.* **2014**, *53*, 12380–12396.
- (72) Galván-Ruiz, M.; Hernández, J.; Baños, L.; Noriega-Montes, J.; Rodríguez-García, M. Characterization of Calcium Carbonate, Calcium Oxide, and Calcium Hydroxide as Starting Point to the Improvement of Lime for Their Use in Construction. *J. Mater. Civ. Eng.* **2009**, *21*, 694–698.
- (73) Finnemore, A.; Cunha, P.; Shean, T.; Vignolini, S.; Guldin, S.; Oyen, M.; Steiner, U. Biomimetic layer-by-layer assembly of artificial nacre. *Nat. Commun.* **2012**, *3*, 966.
- (74) Müller, W. E. G.; Neufurth, M.; Schlossmacher, U.; Schröder, H. C.; Pisignano, D.; Wang, X. The sponge silicatein-interacting protein silintaphin-2 blocks calcite formation of calcareous sponge spicules at the vaterite stage. *RSC Adv.* **2014**, *4*, 2577–2585.
- (75) Natalio, F.; Corrales, T. P.; Panthöfer, M.; Schollmeyer, D.; Lieberwirth, I.; Müller, W. E. G.; Kappl, M.; Butt, H.-J.; Tremel, W. Flexible Minerals: Self-Assembled Calcite Spicules with Extreme Bending Strength. *Science* **2013**, *339*, 1298–1302.
- (76) Balz, M.; Therese, H. A.; Li, J.; Gutmann, J. S.; Kappl, M.; Nasdala, L.; Hofmeister, W.; Butt, H.-J.; Tremel, W. Crystallization of Vaterite Nanowires by the Cooperative Interaction of Tailor-Made Nucleation Surfaces and Polyelectrolytes. *Adv. Funct. Mater.* **2005**, *15*, 683–688.
- (77) Bergström, L.; Sturm, E. V.; Salazar-Alvarez, G.; Cölfen, H. Mesocrystals in Biomaterials and Colloidal Arrays. *Acc. Chem. Res.* **2015**, *48*, 1391–1402.

(78) Dietzsch, M.; Barz, M.; Schüler, T.; Klassen, S.; Schreiber, M.; Susewind, M.; Loges, N.; Hellmann, N.; Fritz, M.; Theato, P.; Fischer, K.; Kühnle, A.; Schmidt, M.; Zentel, R.; Tremel, W.; Lang, M. PAA-PAMPS Copolymers as an Efficient Tool to Control CaCO₃ Scale Formation. *Langmuir* **2013**, *29*, 3080–3088.

(79) Momper, R.; Nalbach, M.; Lichtenstein, K.; Bechstein, R.; Kühnle, A. Stabilization of Polar Step Edges on Calcite (10.4) by the Adsorption of Congo Red. *Langmuir* **2015**, *31*, 7283–7287.

(80) Wang, G.; Li, L.; Lan, J.; Chen, L.; You, J. Biomimetic crystallization of calcium carbonate spherules controlled by hyperbranched polyglycerols. *J. Mater. Chem.* **2008**, *18*, 2789.

(81) Gower, L. B.; Odom, D. J. J. Production and Mechanism of Formation of Monodispersed Hydrosols. *J. Cryst. Growth* **2000**, *210*, 719–734.

(82) Gower, L. B. Polymer-induced liquid precursor (PILP) phases of calcium carbonate formed in the presence of synthetic acidic polypeptides—relevance to biomineralization. *Chem. Rev.* **2008**, *108*, 4551–4627.

(83) Ihli, J.; Kim, Y.-Y.; Noel, E. H.; Meldrum, F. C. The Effect of Additives on Amorphous Calcium Carbonate (ACC): Janus Behavior in Solution and the Solid State. *Adv. Funct. Mater.* **2013**, *23*, 1575–1585.

(84) Ihli, J.; Bots, P.; Kulak, A.; Benning, L. G.; Meldrum, F. C. Elucidating Mechanisms of Diffusion-Based Calcium Carbonate Synthesis Leads to Controlled Mesocrystal Formation. *Adv. Funct. Mater.* **2013**, *23*, 1965–1973.

(85) Ouhenia, S.; Chateigner, D.; Belkhir, M. A.; Guilmeau, E.; Krauss, C. J. Synthesis of calcium carbonate polymorphs in the presence of polyacrylic acid. *J. Cryst. Growth* **2008**, *310*, 2832–281.

(86) Ren, D.; Feng, Q.; Bourrat, X. Effects of additives and templates on calcium carbonate mineralization in vitro. *Micron* **2011**, *42*, 228–245.

(87) Wei, H.; Shen, Q.; Wang, H.; Gao, Y.; Zhao, Y.; Xu, D.; Wang, D. Influence of segmented copolymers on the crystallization and aggregation of calcium carbonate. *J. Cryst. Growth* **2007**, *303*, 537–545.

(88) Yu, J.; Lei, M.; Cheng, B.; Zhao, X. Effects of PAA additive and temperature on morphology of calcium carbonate particles. *J. Solid State Chem.* **2004**, *177*, 681–689.

(89) Wolf, S. E.; Leiterer, J.; Pipich, V.; Barrea, R.; Emmerling, F.; Tremel, W. Strong Stabilization of Amorphous Calcium Carbonate Emulsion by Ovalbumin: Gaining Insight into the Mechanism of ‘Polymer-Induced Liquid Precursor’ Processes. *J. Am. Chem. Soc.* **2011**, *133*, 12642–12649.

(90) Pipich, V.; Balz, M.; Wolf, S.; Tremel, W.; Schwahn, D. Nucleation and Growth of CaCO₃ Mediated by the Egg-White Protein Ovalbumin: A Time-Resolved in situ Study Using Small-Angle Neutron Scattering. *J. Am. Chem. Soc.* **2008**, *130*, 6879–6892.

(91) Long, X.; Nasse, M. J.; Ma, Y.; Qi, L. From synthetic to biogenic Mg-containing calcites: a comparative study using FTIR microspectroscopy. *Phys. Chem. Chem. Phys.* **2012**, *14*, 2255–2263.

(92) Gouadec, G.; Colomban, P. Raman Spectroscopy of nanomaterials: How spectra relate to disorder, particle size and mechanical properties. *Prog. Cryst. Growth Charact. Mater.* **2007**, *53*, 1–56.